# ΔSCF Dyson Orbitals and Pole Strengths from Natural Ionization Orbitals

Hassan Harb and Hrant P. Hratchian[a)]

*Department of Chemistry and Chemical Biology and Center for Chemical Computation and Theory, University of California, Merced, California 95343, USA*

The calculation of photoionization cross-sections can play a key role in spectral assignments using modeling and simulation. In this work, we provide formal relationships between pole strengths, which are proportional to the photoionization cross-section, and terms related to the Natural Ionization Orbital model for ΔSCF calculations. A set of numerical calculations using the developed models is carried out. Pole strength values computed using the two approaches developed for ΔSCF calculations demonstrate excellent agreement with an electron propagator theory model.

**Keywords**: Ionization, Photoelectron Spectroscopy, Natural Ionization Orbitals, Dyson Orbital, Pole Strength, Photoionization Cross-Section

---
[a)]Electronic mail: hhratchian@ucmerced.edu

# I. INTRODUCTION

The study of electron detachment provides a rich space for interrogating the structure of atomic and molecular systems.[1–12] Indeed, modern applications of photodetachment methods such as cryo-SEVI have been used to provide exceptional insight to structure, bonding, and reactivity in an array of molecular systems.[13–18] Modeling electron detachment processes with electronic structure theory is often essential to corroborate experimental results and make spectral assignments. Work from our lab in collaboration with experimental colleagues considering such experiments, for example, has led to detailed understanding of a number of transition metal and inner-transition metal containing systems.[19–25]

Particularly because electron number changes in electron detachment and electron attachment, the quality of electronic structure theory studies of such processes can be quite sensitive to electron correlation treatment.[26–28] Early approaches specifically designed to address this concern implemented wave function models beyond the Hartree–Fock (HF) self–consistent field (SCF) model. These included the Equations of Motion (EOM) approach of Simons[29–34] and the electron propagator theory (EPT) scheme of Cederbaum.[35–38] Those pioneering theory advances subsequently led to two families of modern post-SCF theories: The EOM approach developed ionization potential (IP) and electron affinity (EA) EOM coupled cluster models by Krylov,[39–46] Piecuch,[47–53] and Bartlett.[54–56] Recent advances in EPT include the hierarchy of schemes by Ortiz and co-workers.[57–68]

An alternative approach to computing electron detachment and attachment energies is to straightforwardly evaluate the difference between two stationary state calculations. At the SCF level this gives the $\Delta$SCF approach, which is most commonly employed using Density Functional Theory (DFT) in modern applications. The $\Delta$SCF approach is subject to the inherent limitations of the underlying SCF model chemistry. Nevertheless, for systems with bound initial and final detachment/attachment electronic structures, DFT – as it is in nearly all areas of modern electronic structure theory applications – is the workhorse of $\Delta$SCF. Owing to the inclusion of dynamic electron correlation in approximate functionals, $\Delta$DFT calculations often yield reasonably good agreement with experimental and high-level computational results.

The $\Delta$DFT scheme has a few key additional advantages over post-SCF models. First, the affordability and wide availability of analytic DFT gradient theory readily allows re-

searchers to include geometric relaxation effects to evaluate both vertical and adiabatic detachment/attachment energies. Furthermore, efficient analytic DFT second-derivative codes provide a direct and simple means for including vibrational structure in simulated spectra. As our own work has shown, access to these additional handles is critical for discriminating between spectral candidates and making definitive spectral assignments.[19–24]

A particular advantage of EPT models in electron detachment/attachment studies has been their direct relationship to the Dyson orbital framework. Dyson orbitals, also referred to as generalized overlap amplitudes, are defined as the overlap between $n_{el}$ and $n'_{el} = (n_{el}-1)$ wave functions.[39,42,69–73] The Dyson orbital $\phi^d$ is defined by

$$\phi^d = \sqrt{N} \int \Psi^i_{n_{el}}(\mathbf{x}_1, \mathbf{x}_2, ..., \mathbf{x}_{n_{el}})\Psi^f_{n'_{el}}(\mathbf{x}_2, ..., \mathbf{x}_{n_{el}})d\mathbf{x}_2...d\mathbf{x}_{n_{el}} \tag{1}$$

where the initial and final states are given by $\Psi^i_{n_{el}}$ and $\Psi^f_{n'_{el}}$, respectively. (For the purposes of this work, the wave functions are taken to be real.) The Dyson orbital provides a one-electron orbital description of the source of electron loss/gain. The Dyson picture also provides a formal relationship between theory and observed experimental cross-sections (*vide infra*).[64,74] Namely, the norm of the resulting Dyson orbital of Eq. (1), the pole strength $P_n$, is proportional to the likelihood of transition from a particular orbital and is given by[75]

$$P_n = \int |\phi^d|^2 dx \tag{2}$$

Evaluation of the Dyson orbital from a $\Delta$SCF pair of calculations can be carried out using a corresponding orbital based approach.[71,74,76,77] However, in practice $\Delta$SCF based investigations typically employ Koopmans' theorem when interpreting the electron loss or gain being simulated.[78–81] Critically, the Koopmans' approach ignores electron density relaxation in response to ionization.

A few years ago, our lab proposed the natural ionization orbital (NIO) model to provide such an interpretive tool initially developed for use with $\Delta$SCF calculations.[82] The NIO model utilizes a natural orbital transformation of the difference density formed from the initial (with $N$ electrons) and final (with $N \pm 1$ electrons) SCF solutions. The NIO model has been instrumental in making photodetachment spectral assignments and developing an orbital description of the ionization process that would not have been correct using the Koopmans' theorem framework. Indeed, over the last few years we have employed NIO

analysis in studies of complicated photoelectron spectra of transition metal and lanthanide containing clusters.[20,21,23–25,83,84]

In this report, we develop a formal relationship between the NIO model and the Dyson orbital theory. Importantly, this work establishes a clear and concise connection between the non-zero NIO singular-values and the formal Dyson orbital pole strength. After providing two different derivations of this relationship, the method is numerically demonstrated on a set of seven small molecule electron detachment processes. Comparisons are made between EPT and NIO based Dyson orbitals and pole strengths.

## II.   METHODS

As mentioned, the evaluation of a Dyson orbital in the $\Delta$SCF model can be readily determined using the corresponding orbital approach between occupied one-electron molecular orbitals (MOs) of $n_{el}$ electron and $n_{el} - 1$ electron Slater determinants. That framework was used by Martin and Davidson in 1977 to develop their *corresponding ionization orbitals* model.[71,85] More recently, our lab proposed an orbital description for electron detachment processes studied with $\Delta$SCF approaches based on a natural orbital transformation of the difference density from initial and final states, which we named the NIO model.[82]

While it is a relatively straightforward exercise to show that the corresponding ionization orbital and NIO models both yield a one-electron orbital that is proportional to the $\Delta$SCF Dyson orbital, evaluation of the Dyson orbital pole strength using the NIO model is less clear. With this in mind, this section begins by briefly defining the NIO model. Then, we develop two different derivations for evaluating pole strengths in terms of the NIO model. We note that the remainder of this discussion focuses on electron detachment; analogous expressions can be derived for electron attachment processes.

### A.   Natural Ionization Orbitals

The NIO model provides a compact orbital representation of ionization processes by using the difference of one-particle density matrices and provides a means for interpreting and characterizing electronic detachment processes, including distinguishing between one-electron transitions and shake-up/shake-off transitions.[20,21,23–25] In the case of electron

detachment, the difference density matrix, $\mathbf{\Delta}_P$, can be calculated for a vertical detachment according to

$$\mathbf{\Delta}_P = \mathbf{P}^f - \mathbf{P}^i \tag{3}$$

where $\mathbf{P}^i$ and $\mathbf{P}^f$ are *initial* ground state and *final* ionized state density matrices (which are in the atomic orbital (AO) basis in our implementation). The change in the number of electrons, $\Delta n_{el}$, can be given in terms of the difference density matrix and the AO overlap matrix, $\mathbf{S}$, according to

$$\Delta_{el} = \text{tr}(\mathbf{\Delta}_P \mathbf{S}) \tag{4}$$

where $\text{tr}(\mathbf{X})$ denotes the trace of matrix $\mathbf{X}$.

A set of orbitals, $\phi_P$, can be constructed in the occupation number basis from the canonical MO, $\{\psi_p\}$, according to

$$(\phi_1, \phi_2, ..., \phi_{N_{basis}}) = (\psi_1, \psi_2, ..., \psi_{N_{basis}})\mathbf{U} \tag{5}$$

where the rotation matrix $\mathbf{U}$ can be determined by solving the eigenvalue equation

$$\mathbf{U}^T \mathbf{S}^{1/2} \mathbf{\Delta}_P \mathbf{S}^{1/2} \mathbf{U} = \delta_{elec} \tag{6}$$

In Eq. (6), $\delta_{elec}$ is a diagonal matrix containing the occupation change number for each NIO. The eigenvectors $\mathbf{U}$ can be back-transformed to the AO basis to give the NIO coefficients $\mathbf{V}$ according to

$$\mathbf{V} = \mathbf{S}^{-1/2} \mathbf{U} \tag{7}$$

## B.   NIO Pole Strength Model A: Determinant Approach

Following King et al.,[77] we define $\mathbf{D}$ to be the overlap matrix between occupied MOs of the initial and final SCF solutions,

$$\mathbf{D} = \left(\mathbf{C}^f_{(occ)}\right)^T \mathbf{S} \mathbf{C}^i_{(occ)} \tag{8}$$

where $\mathbf{C}^i_{(occ)}$ and $\mathbf{C}^f_{(occ)}$ are the occupied MO coefficients of initial and final states, respectively. Singular-value decomposition of $\mathbf{D}$ yields

$$\mathbf{D} = \mathbf{Q}\mathbf{\Sigma}\mathbf{R}^T \tag{9}$$

5

The eigenvectors and eigenvalues of the product $\mathbf{D}^T\mathbf{D}$ are given by $\mathbf{R}$ and $\mathbf{\Sigma}^2$,

$$
\begin{aligned}
\mathbf{D}\mathbf{D}^T &= \left(\mathbf{C}^f_{(\text{occ})}\right)^T \mathbf{S}\mathbf{C}^i_{(\text{occ})} \left(\mathbf{C}^i_{(\text{occ})}\right)^T \mathbf{S}\mathbf{C}^f_{(\text{occ})} \\
&= \mathbf{Q}\mathbf{\Sigma}\mathbf{R}^T\mathbf{R}\mathbf{\Sigma}^T\mathbf{Q}^T = \mathbf{Q}\mathbf{\Sigma}^2\mathbf{Q}^T
\end{aligned}
\tag{10}
$$

where $\mathbf{\Sigma}^2$ is used to denote $\mathbf{\Sigma}\mathbf{\Sigma}^T$. Whereas the diagonal matrix of singular values $\mathbf{\Sigma}$ is rectangular, $\mathbf{\Sigma}^2$ is a square diagonal matrix. In the case of electron detachment, the common application of the NIO model used by our lab, the dimension of $\mathbf{\Sigma}^2$ is $n'_{el} = (n_{el} - 1)$.

We note that the initial and final state density matrices are given by

$$
\mathbf{P}^i = \mathbf{C}^i_{(\text{occ})} \left(\mathbf{C}^i_{(\text{occ})}\right)^T
\tag{11}
$$

$$
\mathbf{P}^f = \mathbf{C}^f_{(\text{occ})} \left(\mathbf{C}^f_{(\text{occ})}\right)^T
\tag{12}
$$

Eq. (10) can be rewritten as

$$
\mathbf{D}\mathbf{D}^T = \left(\mathbf{C}^f_{(\text{occ})}\right)^T \mathbf{S}\mathbf{P}^i\mathbf{S}\mathbf{C}^f_{(\text{occ})} = \mathbf{Q}\mathbf{\Sigma}^2\mathbf{Q}^T
\tag{13}
$$

Using Eq. (3) gives

$$
\left(\mathbf{C}^f_{(\text{occ})}\right)^T \mathbf{S}\left(\mathbf{P}^f - \mathbf{\Delta}_P\right)\mathbf{S}\mathbf{C}^f_{(\text{occ})} = \mathbf{Q}\mathbf{\Sigma}^2\mathbf{Q}^T
\tag{14}
$$

and

$$
\begin{aligned}
\left(\mathbf{C}^f_{(\text{occ})}\right)^T \mathbf{S}\mathbf{C}^f_{(\text{occ})} \left(\mathbf{C}^f_{(\text{occ})}\right)^T \mathbf{S}\mathbf{C}^f_{(\text{occ})} - \\
\left(\mathbf{C}^f_{(\text{occ})}\right)^T \mathbf{S}\mathbf{\Delta}_P\mathbf{S}\mathbf{C}^f_{(\text{occ})} = \mathbf{Q}\mathbf{\Sigma}^2\mathbf{Q}^T
\end{aligned}
\tag{15}
$$

Given that the occupied canonical MOs form an orthonormal set, Eq. (15) becomes

$$
\mathbf{I}_{n'_{el}} - \left(\mathbf{C}^f_{(\text{occ})}\right)^T \mathbf{S}\mathbf{\Delta}_P\mathbf{S}\mathbf{C}^f_{(\text{occ})} = \mathbf{Q}\mathbf{\Sigma}^2\mathbf{Q}^T
\tag{16}
$$

where $\mathbf{I}_{n'_{el}}$ is the identity matrix with dimension $(n'_{el} \times n'_{el})$.

Given that $\mathbf{U}$ is unitary, Eq. (6) can be used to write Eq. (16) as

$$
\mathbf{I}_{n'_{el}} - \left(\mathbf{C}^f_{(\text{occ})}\right)^T \mathbf{S}^{1/2}\mathbf{U}\delta_{elec}\mathbf{U}^T\mathbf{S}^{1/2}\mathbf{C}^f_{(\text{occ})} = \mathbf{Q}\mathbf{\Sigma}^2\mathbf{Q}^T
\tag{17}
$$

Using Eq. (7) gives

$$
\mathbf{I}_{n'_{el}} - \left(\mathbf{C}^f_{(\text{occ})}\right)^T \mathbf{S}\mathbf{V}\delta_{elec}\mathbf{V}^T\mathbf{S}\mathbf{C}^f_{(\text{occ})} = \mathbf{Q}\mathbf{\Sigma}^2\mathbf{Q}^T
\tag{18}
$$

which we rewrite as

$$
\mathbf{T}_{(\text{occ})}\delta_{elec}\mathbf{T}^T_{(\text{occ})} = \mathbf{I}_{n'_{el}} - \mathbf{Q}\mathbf{\Sigma}^2\mathbf{Q}^T
\tag{19}
$$

Elements of $\mathbf{T}$ expand the NIOs in the final state MO basis,

$$T_{p\alpha} = \sum_{\mu\nu} C^f_{\mu p} S_{\mu\nu} V_{\nu\alpha} \tag{20}$$

where $\{\mu, \nu, \cdots\}$ denote atomic orbital basis functions, $\{p, q, \cdots\}$ denote molecular orbitals, and $\{\alpha, \beta, \cdots\}$ denote NIOs. Note that the rectangular matrix $\mathbf{T}_{(\mathrm{occ})}$ in Eq. (19) only includes expansion coefficients of Eq. (20) in the final state *occupied* MO sub-space.

Multiplying Eq. (19) on the left by $\mathbf{Q}^T$ and on the right by $\mathbf{Q}$ gives

$$\mathbf{Q}^T \mathbf{T}_{(\mathrm{occ})} \delta_{elec} \mathbf{T}^T_{(\mathrm{occ})} \mathbf{Q} = \mathbf{Q}^T \mathbf{I}_{n'_{el}} \mathbf{Q} - \mathbf{Q}^T \mathbf{Q} \mathbf{\Sigma}^2 \mathbf{Q}^T \mathbf{Q} \tag{21}$$

Given that $\mathbf{Q}$ is unitary, Eq. (21) simplifies to

$$\mathbf{\Sigma}^2 = \mathbf{I}_{n'_{el}} - \mathbf{Q}^T \mathbf{T}_{(\mathrm{occ})} \delta_{elec} \mathbf{T}^T_{(\mathrm{occ})} \mathbf{Q} \tag{22}$$

Following King et al.,[77] the square of the overlap of the initial and final state Slater determinants, i.e. the pole strength, is given by $\det(\Sigma^2)$. Thus,

$$\det\left(\mathbf{\Sigma}^2\right) = \det\left(\mathbf{I}_{n'_{el}} - \mathbf{Q}^T \mathbf{T}_{(\mathrm{occ})} \delta_{elec} \mathbf{T}^T_{(\mathrm{occ})} \mathbf{Q}\right) \tag{23}$$

Therefore, the right-hand side of Eq. (23) also gives the overlap of these two Slater determinants, which will ultimately provide a means to calculate the pole strength associated with the Dyson orbital. Using Sylvester's determinant theorem,[86–89] Eq. (23) can be rewritten as

$$\det\left(\mathbf{\Sigma}^2\right) = \det\left(\mathbf{I}_{N_{basis}} - \mathbf{T}^T_{(\mathrm{occ})} \mathbf{T}_{(\mathrm{occ})} \delta_{elec}\right) \tag{24}$$

which provides a form for the pole strength that can be directly evaluated using terms formed in the NIO model according to

$$P_n = \det\left(\mathbf{I}_{N_{basis}} - \mathbf{T}^T_{(\mathrm{occ})} \mathbf{T}_{(\mathrm{occ})} \delta_{elec}\right) \tag{25}$$

## C.  NIO Pole Strength Model B: Trace Approach

The NIO model often yields only one non-zero eigenvalue corresponding to the one-electron Dyson orbital. However, in many cases the SCF determinant undergoes relaxation upon ionization relative to the converged initial state determinant. Under such conditions, the NIO analysis yields one or more pairs of fractional occupation change eigenvalues. Most

common are cases with only one fractional NIO eigenvalue pair with appreciable magnitudes. Under such conditions, an approximate second approach for computing pole strengths from the NIO model can be developed.

The development of this approximate second model begins by taking the trace of Eq. (19) to give

$$\text{tr}\big(\mathbf{T}_{(occ)}\delta_{elec}\mathbf{T}_{(occ)}^T\big) = \text{tr}\big(\mathbf{I}_{n'_{el}} - \mathbf{Q}\mathbf{\Sigma}^2\mathbf{Q}^T\big) \tag{26}$$

Applying the cyclic rule of traces $\text{tr}(\mathbf{ABC}) = \text{tr}(\mathbf{BCA}) = \text{tr}(\mathbf{CAB})$, recalling that $\mathbf{QQ}^T = \mathbf{I}_{n'_{el}}$, and noting $\text{tr}(\mathbf{I}_{n'_{el}}) = n'_{el} = n_{el} - 1$ yield

$$\text{tr}\big(\mathbf{\Sigma}^2\big) = n_{el} - 1 - \text{tr}\big(\delta_{elec}\mathbf{T}_{(occ)}^T\mathbf{T}_{(occ)}\big) \tag{27}$$

Assuming no more than one corresponding orbital pair has an overlap less than 1, the trace of $\mathbf{\Sigma}^2$ is given by

$$\text{tr}\big(\mathbf{\Sigma}^2\big) = n_{el} - 2 + \sigma^2 \tag{28}$$

where $\sigma^2$ is the diagonal element of $\mathbf{\Sigma}^2$ associated with the single fractional-overlap corresponding orbital. Since $\mathbf{\Sigma}^2$ is diagonal and all other elements are equal to 1, the pole strength under this condition is equal to $\sigma^2$. Using Eqs. (27) and (28) gives an alternative and approximate expression for the $\Delta$SCF pole strength using the NIO model as

$$P_n = \sigma^2 = 1 - \text{tr}\big(\delta_{elec}\mathbf{T}_{(occ)}^T\mathbf{T}_{(occ)}\big) \tag{29}$$

## III. NUMERICAL TESTS

Numerical tests of NIO based pole strengths have been carried out on a set of seven verticle electron detachment processes. Electronic structure calculations were performed using a local development version of the Gaussian suite of programs.[90] The unrestricted HF method was used in all cases and the stability of all HF determinants was verified.[91,92] Initial state geometries were optimized using standard methods.[93] Ionization energies calculated from $\Delta$SCF and EPT methods are sown in the supporting information. While ionization potentials obtained with $\Delta$SCF are lower than those obtained using EPT, we highlight that the aim of this study focuses on presenting the relationship between NIOs and Dyson orbitals rather than assessing the validities of ionization energies obtained using $\Delta$SCF and EPT.

NIO analyses were performed using an open source code.[94] For each studied detachment, orbital occupation change numbers are reported ($\delta_{elec}$). In the cases where reasonable orbital

TABLE I. Pole strengths calculated using EPT, NIO trace, and NIO Determinant methods.

| Molecule | NIO (Determinant)[a] | NIO (Trace)[b] | EPT |
|---|---|---|---|
| Formaldehyde | 0.907 | 0.906 | 0.925 |
| Nitromethyl Radical | 0.847 | 0.845 | 0.911 |
| $H_2O$ | 0.948 | 0.948 | 0.933 |
| Chlorobenzene | 0.897 | 0.895 | 0.901 |
| $CCl_4$ | 0.933 | 0.933 | 0.913 |
| $NH_3$ | 0.947 | 0.946 | 0.927 |
| Ethanol | 0.929 | 0.927 | 0.922 |

[a] See Eq. (25).
[b] See Eq. (29).

relaxation is observed, the projection of the orbitals onto the occupied manifold of the initial state (%occ) is also reported. We note that % occ is calculated using an approach similar to Eq. 20. In lieu of projecting the NIOs onto the final occupied state manifold, we project the NIO coefficients onto the *initial state* MOs followed by considering the subspace that maps onto the *occupied* manifold of the initial state.

NIO based pole strengths from $\Delta$SCF calculations were compared to results from EPT diagonal self-energy approximation calculations.[75] Table I provides a comparison of pole strengths obtained from both the $\Delta$SCF/NIO and EPT approaches. Tables S2 and S3 report $\langle S^2 \rangle$ and detachment energies for the HF and EPT calculations used in this work. Consistent with previous reports, HF theory with a modest basis set yields only modest agreement between vertical detachment energies evaluated using the $\Delta$SCF approach and higher levels of theory.[95,96] Nitromethyl radical exhibits a high degree of spin contamination and correspondingly poor $\Delta$SCF vertical detachment energy. Nevertheless, as shown below, the chosen model chemistries are adequate for demonstrating the formal relationships for evaluating pole strengths developed above.

## A.  Formaldehyde

The first system considered is the valence electron detachment from the $^1A_1$ ground state of formaldehyde. The result is the $^2B_2$ state. The NIO analysis was carried out using a $\Delta$SCF calculation performed at the UHF/6-311++G level of theory. Figure 1 shows the $\Delta$SCF Dyson orbtial (the NIO with eigenvalue $-1.0$, depicting the electron hole) on the left and the Dyson orbital calculated using the EPT diagonal self-energy approximation on the right. In this case, it is clear that the $\Delta$SCF and EPT based Dyson orbitals are qualitatively the same.



**ΔSCF Dyson**
**($\delta_{elec}$ = -1.0)**
**UEPT Dyson**
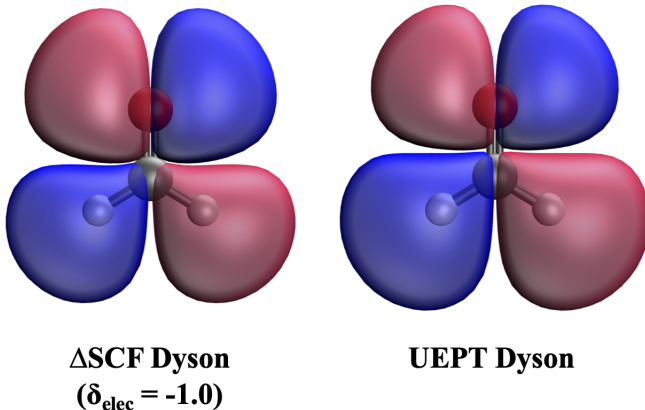
FIG. 1. $\Delta$SCF (left) and EPT (right) Dyson orbitals associated with electron detachment of $^1A_1$ ground-state of formaldehyde.

This first numerical example shows very good agreement between the NIO and EPT approaches for calculating Dyson orbital pole strength. The NIO model suggests minimal electron relaxation with small pairs of occupation change numbers ($|\delta_{elec}| < 0.2$), which yields a large pole strength. Using the NIO analysis yields $\Delta$SCF pole strengths of 0.907 and 0.906 from the determinant and trace approaches, respectively. The EPT pole strength, $P_n$, is 0.925. The difference between the $\Delta$SCF and EPT based values is roughly 2%.

## B.  Nitromethyl Radical

Calculations on the nitromethyl radical were carried out using the UHF/6-31g(3d,3p) model chemistry. Electron detachment from the ground state of the nitromethyl radical

$(^1A' \leftarrow \, ^2A'')$ involves a meaningful degree of accompanying electron relaxation. As shown in the top panel of Fig. 2, the $\Delta$SCF and EPT Dyson orbitals are essentially the same. Unlike the previous example case (formaldehyde), detachment from the nitromethyl radical results in meaningful orbital relaxation. As shown in in the boxed bottom panel of Fig. 2, there are two pairs of relaxation NIOs (one $\alpha$ pair and one $\beta$ pair).
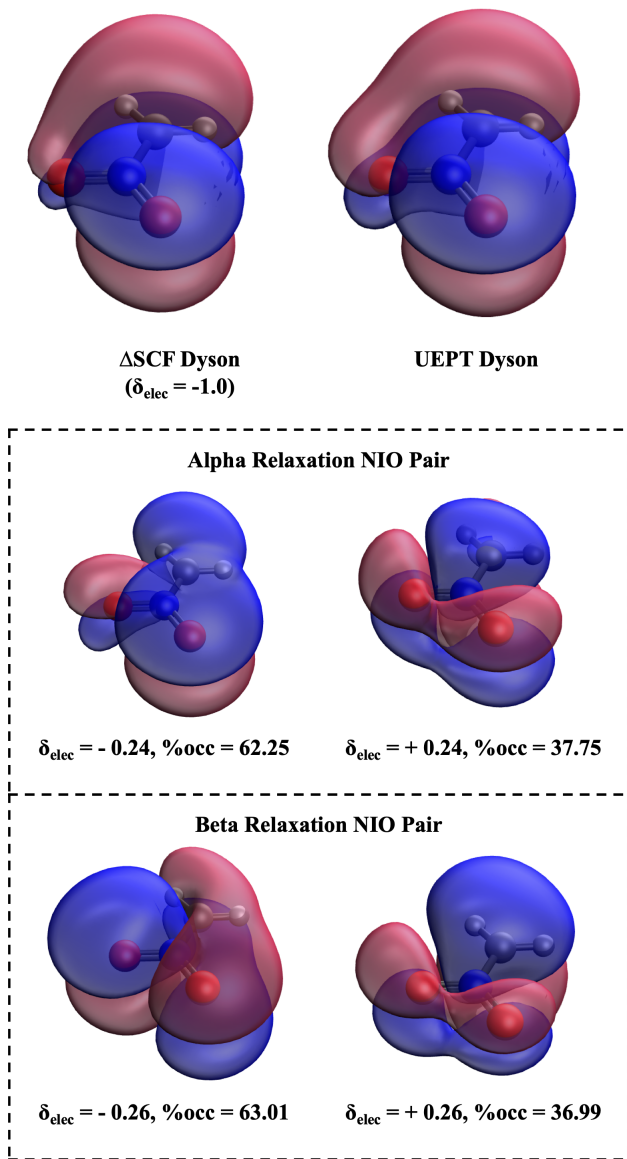


FIG. 2. $\Delta$SCF (top left) and EPT (top right) Dyson orbitals associated with electron detachment from ground state nitromethyl radical. Dashed boxes present the relaxation NIO pairs.

Projections onto the initial state occupied and virtual MO sub-spaces (or, equivalently, final state virtual and occupied MO sub-spaces) of relaxation NIO pairs show complemen-

tarity in their occupied/virtual decomposition. For example, the $\alpha$ relaxation NIO pair has initial state occupied MO projections of 62.3% and 37.8%. The $\beta$ relaxation NIO pair has initial state occupied MO projections of 63.0% and 36.0%. The negative $\alpha$ relaxation NIO is 62.25% occupied in the initial state and the positive eigenvalue NIO constitutes of 37.75% of the initial occupied manifold. Similarly, the $\beta$ relaxation NIO pair is associated with eigenvalues of $\delta_{elec} = \pm 0.26$. The positive eigenvalue NIO has a 63.01% occupied character and the negative-eigenvalue NIO has a 36.00% occupied character.

In previous work, we hypothesized that non-zero fractional change eigenvalues in the NIO analysis correspond to decreased pole strengths.[20] This work quantifies that relationship though Eqs. (25) and (29). Indeed, as shown in Table I the relaxation NIOs decrease the pole strength to $\sim 0.85$ in the $\Delta$SCF model and $\sim 0.91$ in the EPT diagonal self-energy approximation. Notably, the approximate trace method of Eq. (29) is quite close to the exact $\Delta$SCF pole strength result. The difference between the two $\Delta$SCF methods is less than 0.5%. This test case presents the largest disagreement in calculated pole strengths between $\Delta$SCF and EPT models. As noted previously, NIOs based on spin-unrestricted calculations do account for both orbital relaxation and some electron correlation contributions, but the unrestricted framework does introduce spin contamination.[82] In this particular case, the values of $\langle S^2 \rangle$ are 1.17 and 0.92 for the doublet and singlet states, respectively.

## C. Water

The third system included in the test set is the electron detachment from the $^1A_1$ ground-state of water using the UHF/6-311G** model chemistry. Figure 3 shows the $\Delta$SCF (left) and EPT (right) Dyson orbitals for $^1A_1 \rightarrow \, ^2B_1 + e^-$ detachment of water. As shown, these two approaches for evaluating electron detachment result in similar Dyson orbitals. NIO analysis shows three pairs of relaxation NIOs orbitals with very small electron change eigenvalues ($|\delta_{elec}| < 0.1$). The calculated $\Delta$SCF pole strength using the NIO determinant and trace approaches is 0.948, which is only 1.68% different from the EPT diagonal self-energy pole strength.
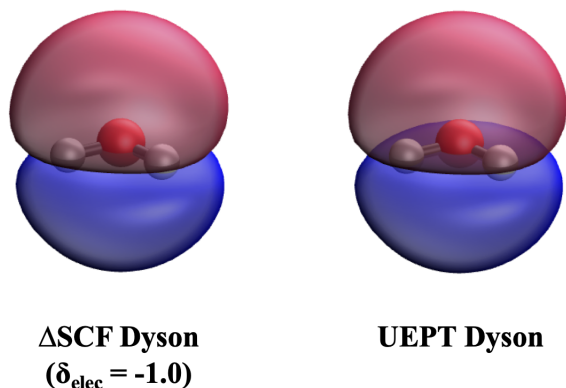
**ΔSCF Dyson**
**($\delta_{elec}$ = -1.0)**

**UEPT Dyson**

FIG. 3. ΔSCF (left) and EPT (right) Dyson orbitals associated with electron detachment of $^1A_1$ ground state of water.

## D.  Chlorobenzene

A second case in the test set exhibiting significant orbital relaxation with electronic detachment is the ionization of chlorobenzene. The ΔSCF and EPT calculations were run using the UHF/6-311G(d,p) level of theory. Figure 4 shows the computed Dyson orbitals associated with the $^2B_1 \leftarrow {}^1A_1$ detachment of $C_6H_5Cl$. As with the previous examples, the ΔSCF and EPT Dyson orbitals closely resemble each other, describing electron detachment from a delocalized $\pi^*$ orbital.

The NIO analysis shows a relaxation pair with electron occupation change eigenvalues of $\pm 0.21$, as shown in the bottom panel of Fig. 4. The orbital with a negative fractional occupation change has a 60.75% contribution from the initial state occupied MOs, while its complimentary relaxation NIO has a 39.25% contribution from the initial state occupied MOs. Two additional minor relaxation NIO pairs (not shown in Fig. 4) were found with occupation change values of $\pm 0.12$. As discussed above for the nitromethyl radical case, relaxation NIOs correspond to decreased pole strengths. Using the determinant and trace approaches, the calculated ΔSCF pole strengths are 0.895 and 0.897, respectively. Both values agree well with the EPT pole strength of 0.901.

**ΔSCF Dyson**
**($δ_{elec}$ = -1.0)**

**UEPT Dyson**

**Alpha Relaxation NIO Pair**

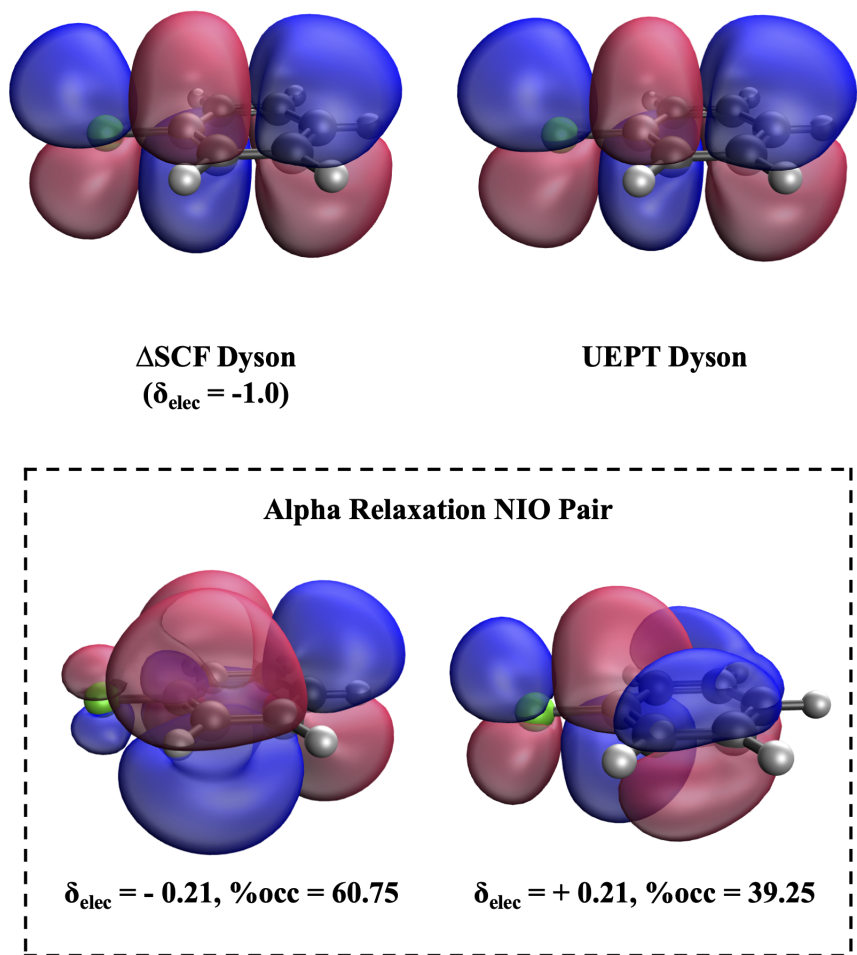$δ_{elec}$ = - 0.21, %occ = 60.75          $δ_{elec}$ = + 0.21, %occ = 39.25

FIG. 4. ΔSCF (top left) and EPT (top right) Dyson orbitals associated with electron detachment from chlorobenzene. The dashed box presents the relaxation NIO pair.

### E.    Tetrachloromethane

Calculations on the vertical electron detachment energy for tetrachloromethane were carried out using the UHF/6-311G(d,p) level of theory. The ΔSCF and EPT Dyson orbitals corresponding to detachment from the $^1A$ ground state to the $^2A$ cation are shown in Fig. 5. Unlike the previous cases, there is a noticeable difference between the ΔSCF an EPT Dyson orbitals. This difference is due to the lack of symmetry in the cation SCF wave function. Neutral tetrachloromethane features a triply-degenerate highest-occupied molecular orbital (HOMO). The EPT method is able to correctly predict a symmetric description of the Dyson orbtial due to symmetry adaptation, which the ΔSCF model does not include. Notably, the degree of spin contamination in the cation – which one might expect to be meaningful – is

quite modest with $\langle S^2 \rangle = 0.76$. As shown in Fig. 5, the $\Delta$SCF Dyson orbital does share key features with the EPT Dyson orbital. The Dyson orbitals for each model are similarly delocalized and have the same general nodal structure. NIO analysis showed minor electron relaxation with two non-trivial relaxation NIO pairs with $\delta_{elec} = \pm 0.11$ and $\pm 0.13$. The resulting $\Delta$SCF pole strength is 0.933 using both determinant and trace NIO approaches. The value is in very good agreement with the EPT pole strength of the detachment (0.927).
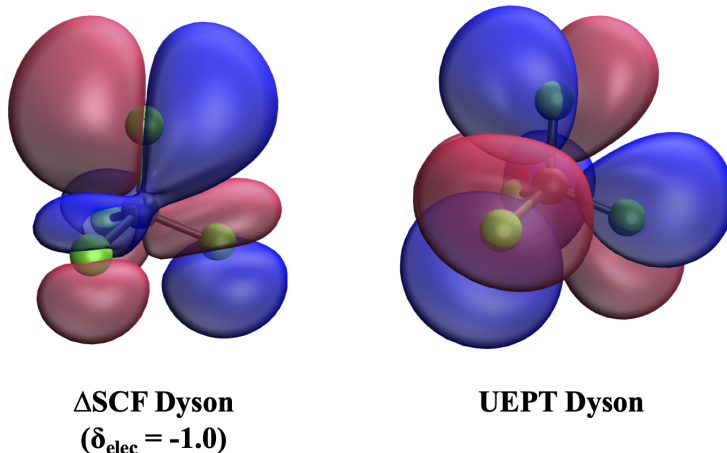


**$\Delta$SCF Dyson**
**($\delta_{elec}$ = -1.0)**

**UEPT Dyson**

FIG. 5. $\Delta$SCF (left) and EPT (right) Dyson orbitals associated with electron detachment from the ground state of tetrachloromethane.

## F.   Ammonia

The detachment from ground state of ammonia ($^1A_1$) shows a Koopmans-like behavior. Both $\Delta$SCF and EPT Dyson orbitals (Fig. 6) show that the detached electron originates from the $2a_1$ nitrogen lone pair orbital. In addition, NIO analysis showed only very slight orbital relaxation, with the most meaningful relaxation NIO pairs given by $\delta_{elec} \pm 0.11$. Calculations of pole strengths using the determinant and trace approaches yield values of 0.947 and 0.946, respectively. These values are very close to the EPT pole strength (0.927), with a difference of only  2%.
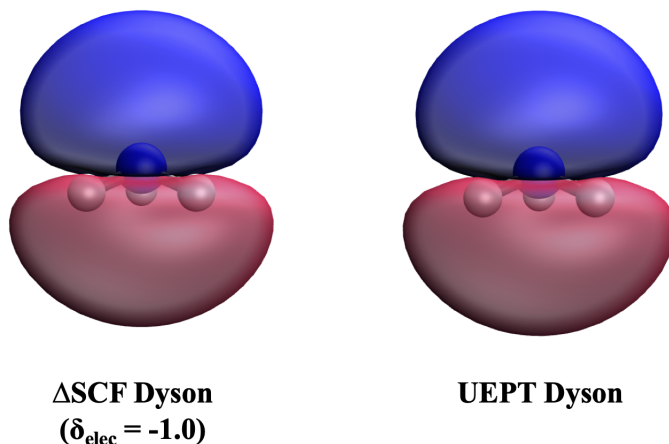
**ΔSCF Dyson**
**($\delta_{elec}$ = -1.0)**

**UEPT Dyson**

FIG. 6. ΔSCF (left) and EPT (right) Dyson orbitals associated with electron detachment from the ground state of $NH_3$.

## G. Ethanol

The final case considered in the test set electron detachment from the ground state of ethanol to form the $^2A$ radical cation. For this test, the UHF/6-311G** level of theory was employed. The ΔSCF and EPT Dyson orbitals are shown in Fig. 7. Both orbitals indicate electron detachment from a non-bonding MO. However, the ΔSCF Dyson orbital is more localized on the C−O bond, while the EPT Dyson orbital is delocalized over the whole molecule. The ΔSCF pole strengths calculated using determinant (0.929) and trace (0.927) approaches are in excellent agreement with the EPT pole strength (0.922).

## IV. CONCLUSION

This work presented two formulations relating Dyson orbital pole strength in ΔSCF calculations using the NIO model. The relationships described in Eqs. (25) and (29) show that the occupation change numbers obtained from an NIO analysis relate to the overlap of the initial and final SCF states of electron detachment. Comparisons of Dyson orbitals and their pole strengths calculated using ΔSCF and EPT approaches were also presented. It was shown that using the NIO model, ΔSCF Dyson orbitals and pole strengths are often in excellent agreement with EPT results.
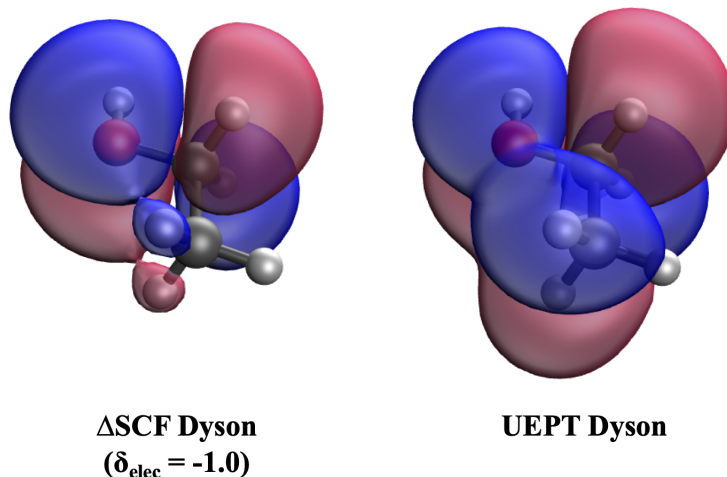
**ΔSCF Dyson**
**($\delta_{elec}$ = -1.0)**

**UEPT Dyson**

FIG. 7. ΔSCF (left) and EPT (right) Dyson orbitals associated with electron detachment from the ground state of ethanol.

## ACKNOWLEDGMENTS

## SUPPLEMENTARY INFORMATION

See supplementary material for SCF energies for reported ground and detached states, $\langle S^2 \rangle$, and vertical detachment energies calculated using ΔSCF and EPT methods, and optimized geometries.

## DATA AVAILABILITY

The data that support the findings of this study are available from the corresponding author upon reasonable request.

# REFERENCES

[1] S. E. Waller, J. E. Mann, D. W. Rothgeb, and C. C. Jarrold, "Study of $MoNbO_y$ (y=2-5) anion and neutral clusters using photoelectron spectroscopy and density functional theory calculations: impact of spin contamination on single point calculations." J. Phys. Chem. A **116**, 9639–9652 (2012).

[2] S. E. Waller, M. Ray, B. L. Yoder, and C. C. Jarrold, "Simple relationship between oxidation state and electron affinity in gas-phase metal–oxo complexes," J. Phys. Chem. A **117**, 13919–13925 (2013).

[3] C. C. Jarrold, B. L. Yoder, J. T. Maze, and K. Raghavachari, "Structures of $Mo_2O_y^-$ and $Mo_2O_y$ (y=2, 3 and 4) studied by anion photoelectron spectroscopy and density functional theory calculations," J. Chem. Phys. **122**, 094313 (2005).

[4] J. E. Mann, D. W. Rothgeb, S. E. Waller, and C. C. Jarrold, "Study of $MoVO_y$ (y=2-5) anion and neutral clusters using anion photoelectron spectroscopy and density functional theory calculations," J. Phys. Chem. A **114**, 11312–11321 (2010).

[5] N. J. Mayhall, D. W. Rothgeb, E. Hossain, K. Raghavachari, and C. C. Jarrold, "Electronic structures of $MoWO_y^-$ and $MoWO_y$ determined by anion photoelectron spectroscopy and DFT calculations," J. Chem. Phys. **130**, 124313 (2009).

[6] M. F. A. Hendrickx and V. T. Tran, "On the electronic and geometric structures of $FeO_2^{-/0}$ and the assignment of the anion photoelectron spectrum," J. Chem. Theory Comput. **8**, 3089–3096 (2012).

[7] M. F. A. Hendrickx and K. R. Anam, "A new proposal for the ground state of the $FeO^-$ cluster in the gas phase and for the assignment of its photoelectron spectra." J. Phys. Chem. A **113**, 8746–8753 (2009).

[8] V. T. Tran and M. F. A. Hendrickx, "Description of the geometric and electronic structures responsible for the photoelectron spectrum of $FeO_4^-$," J. Chem. Phys. **135**, 094505 (2011).

[9] G. Meloni, M. J. Ferguson, and D. M. Neumark, "Negative ion photodetachment spectroscopy of the $Al_3O_2$, $Al_3O_3$, $Al_4O_x$, $Al_5O_x$ (x=3-5), $Al_6O_5$, and $Al_7O_5$ clusters," Phys. Chem. Chem. Phys. **5**, 4073 (2003).

[10] J. B. Kim, M. L. Weichman, and D. M. Neumark, "Structural isomers of $Ti_2O_4$ and $Zr_2O_4$ anions identified by slow photoelectron velocity-map imaging spectroscopy," J. Am. Chem. Soc. **136**, 7159–7168 (2014).

[11] J. B. Kim, M. L. Weichman, and D. M. Neumark, "High-resolution anion photoelectron spectra of $TiO_2^-$, $ZrO_2^-$, and $HfO_2^-$ obtained by slow electron velocity-map imaging." Phys. Chem. Chem. Phys. **15**, 20973–20981 (2013).

[12] G. Meloni, S. M. Sheehan, and D. M. Neumark, "Gallium oxide and dioxide: investigation of the ground and low-lying electronic states via anion photoelectron spectroscopy." J. Chem. Phys. **122**, 074317 (2005).

[13] H. Timmers, X. Zhu, Z. Li, Y. Kobayashi, M. Sabbar, M. Hollstein, M. Reduzzi, T. J. Martínez, D. M. Neumark, and S. R. Leone, "Disentangling conical intersection and coherent molecular dynamics in methyl bromide with attosecond transient absorption spectroscopy," Nat. Commun. **10**, 1–8 (2019).

[14] M. L. Weichman and D. M. Neumark, "Slow photoelectron velocity-map imaging of cryogenically cooled anions," Annu. Rev. Phys. Chem. **69**, 101–124 (2018).

[15] M. C. Heaven and K. A. Peterson, "Probing actinide bonds in the gas phase: Theory and spectroscopy," Exp. Theor. Approaches Actinide Chem. , 1 (2018).

[16] M. C. Heaven, "Spectroscopy and dynamics of open-shell van der waals molecules," Annu. Rev. Phys. Chem. **43**, 283–310 (1992).

[17] W. H. Robertson and M. A. Johnson, "Molecular aspects of halide ion hydration: The cluster approach," Annu. Rev. Phys. Chem. **54**, 173–213 (2003).

[18] B. C. Garrett, D. A. Dixon, D. M. Camaioni, D. M. Chipman, M. A. Johnson, C. D. Jonah, G. A. Kimmel, J. H. Miller, T. N. Rescigno, P. J. Rossky, *et al.*, "Role of water in electron-initiated processes and radical chemistry: Issues and scientific advances," Chem. Rev. **105**, 355–390 (2005).

[19] L. M. Thompson and H. P. Hratchian, "Modeling the Photoelectron Spectra of $MoNbO_2^-$ accounting for spin contamination in density functional theory." J. Phys. Chem. A **119**, 8744–8751 (2015).

[20] L. M. Thompson, C. C. Jarrold, and H. P. Hratchian, "Explaining the $MoVO_4^-$ photoelectron spectrum: Rationalization of geometric and electronic structure," J. Chem. Phys. **146**, 104301 (2017).

[21] J. A. DeVine, A. Abou Taka, M. C. Babin, M. L. Weichman, H. P. Hratchian, and D. M. Neumark, "High-resolution photoelectron spectroscopy of $TiO_3H_2^-$: Probing the $TiO_2^-$ + $H_2O$ dissociative adduct," J. Chem. Phys. **148**, 222810 (2018).

[22] J. E. Topolski, J. O. Kafader, V. Marrero-Colon, S. S. Iyengar, H. P. Hratchian, and C. C. Jarrold, "Exotic electronic structures of $Sm_xCe_{3-x}O_y$ (x= 0-3; y= 2-4) clusters and the effect of high neutral density of low-lying states on photodetachment transition intensities," J. Chem. Phys. **149**, 054305 (2018).

[23] J. L. Mason, H. Harb, J. E. Topolski, H. P. Hratchian, and C. C. Jarrold, "A tale of two stabilities: How one boron atom affects a switch in bonding motifs in $CeO_2B_x^-$ (x= 2, 3) complexes," J. Phys. Chem. A **122**, 9879–9885 (2018).

[24] J. L. Mason, H. Harb, C. D. Huizenga, J. C. Ewigleben, J. E. Topolski, H. P. Hratchian, and C. C. Jarrold, "Electronic and molecular structures of the $CeB_6$ monomer," J. Phys. Chem. A **123**, 2040–2048 (2019).

[25] J. L. Mason, H. Harb, J. E. Topolski, H. P. Hratchian, and C. C. Jarrold, "Exceptionally complex electronic structures of lanthanide oxides and small molecules," Acc. Chem. Res. **52**, 3265–3273 (2019).

[26] J. Simons and W. D. Smith, "Theory of electron affinities of small molecules," J. Chem. Phys. **58**, 4899–4907 (1973).

[27] J. Simons, "Theoretical studies of negative molecular ions," Annu. Rev. Phys. Chem. **28**, 15–45 (1977).

[28] J. E. Mayer, "Electron correlation," Phys. Rev. **100**, 1579 (1955).

[29] J. Simons and P. Jorgensen, "Perturbative solution of equations of motion for excitation and ionization processes," J. Chem. Phys. **64**, 1413–1418 (1976).

[30] J. Simons, "A note on differences between operator-level and function-level equations ol motion," Int. J. Quantum Chem. **12**, 227–229 (1977).

[31] E. Dalgaard and J. Simons, "Equations-of-motion formulation of many-body perturbation theory," J. Phys. B: At. Mol. Phys. **10**, 2767 (1977).

[32] J. Simons, "Equations of motion (eom) methods for computing electron affinities," Encyclopedia of Computational Chemistry (2002).

[33] J. Simons, "Equations of motion methods for computing electron affinities and ionization potentials," in *Theory and Applications of Computational Chemistry* (Elsevier, 2005) pp. 443–464.

[34] J. Simons, "Equations of motion theory for electron affinities," Collect. Czech. Chem. Commun. **70**, 579–604 (2005).

[35] W. von Niessen, J. Schirmer, and L. S. Cederbaum, "Computational methods for the one-particle green's function," Comput. Phys. Rep. **1**, 57–125 (1984).

[36] J. Schirmer, L. Cederbaum, and O. Walter, "New approach to the one-particle green's function for finite fermi systems," Phys. Rev. A **28**, 1237 (1983).

[37] L. Cederbaum, "One-body green's function for atoms and molecules: theory and application," J. Phys. B: At. Mol. Phys. **8**, 290 (1975).

[38] L. S. Cederbaum and J. Zobeley, "Ultrafast charge migration by electron correlation," Chem. Phys. Lett. **307**, 205–210 (1999).

[39] C. M. Oana and A. I. Krylov, "Dyson orbitals for ionization from the ground and electronically excited states within equation-of-motion coupled-cluster formalism: theory, implementation, and examples." J. Chem. Phys. **127**, 234106 (2007).

[40] P. A. Pieniazek, E. J. Sundstrom, S. E. Bradforth, and A. I. Krylov, "Degree of initial hole localization/delocalization in ionized water clusters." J. Phys. Chem. A **113**, 4423–4429 (2009).

[41] C. M. Oana and A. I. Krylov, "Cross sections and photoelectron angular distributions in photodetachment from negative ions using equation-of-motion coupled-cluster Dyson orbitals." J. Chem. Phys. **131**, 124114 (2009).

[42] S. Gozem, A. O. Gunina, T. Ichino, D. L. Osborn, J. F. Stanton, and A. I. Krylov, "Photoelectron wave function in photoionization: plane wave or Coulomb wave?" J. Phys. Chem. Lett. **6**, 4532–4540 (2015).

[43] T.-C. Jagau and A. I. Krylov, "Characterizing metastable states beyond energies and lifetimes: Dyson orbitals and transition dipole moments." J. Chem. Phys. **144**, 054113 (2016).

[44] K. Bravaya, O. Kostko, S. Dolgikh, A. Landau, M. Ahmed, and A. I. Krylov, "Electronic structure and spectroscopy of nucleic acid bases: ionization energies, ionization-induced structural changes, and photoelectron spectra." J. Phys. Chem. A **114**, 12305–12317 (2010).

[45] A. I. Krylov, "The quantum chemistry of open-shell species," Rev. Comput. Chem. **30**, 151–224 (2017).

[46] A. I. Krylov, "Equation-of-motion coupled-cluster methods for open-shell and electronically excited species: The hitchhiker's guide to fock space," Annu. Rev. Phys. Chem. **59** (2008).

[47] K. Kowalski and P. Piecuch, "The active-space equation-of-motion coupled-cluster methods for excited electronic states: The eomccsdt approach," J. Chem. Phys. **113**, 8490–8502 (2000).

[48] K. Kowalski and P. Piecuch, "The active-space equation-of-motion coupled-cluster methods for excited electronic states: Full eomccsdt," J. Chem. Phys. **115**, 643–651 (2001).

[49] J. R. Gour, P. Piecuch, and M. Włoch, "Active-space equation-of-motion coupled-cluster methods for excited states of radicals and other open-shell systems: Ea-eomccsdt and ip-eomccsdt," J. Chem. Phys. **123**, 134113 (2005).

[50] J. R. Gour, P. Piecuch, and M. Włoch, "Extension of the active-space equation-of-motion coupled-cluster methods to radical systems: The ea-eomccsdt and ip-eomccsdt approaches," Int. J. Quantum Chem. **106**, 2854–2874 (2006).

[51] J. R. Gour and P. Piecuch, "Efficient formulation and computer implementation of the active-space electron-attached and ionized equation-of-motion coupled-cluster methods," J. Chem. Phys. **125**, 234107 (2006).

[52] K. Kowalski and P. Piecuch, "New type of noniterative energy corrections for excited electronic states: Extension of the method of moments of coupled-cluster equations to the equation-of-motion coupled-cluster formalism," J. Chem. Phys. **115**, 2966–2978 (2001).

[53] P. Piecuch, K. Kowalski, I. S. Pimienta, and M. J. Mcguire, "Recent advances in electronic structure theory: Method of moments of coupled-cluster equations and renormalized coupled-cluster approaches," Int. Rev. Phys. Chem. **21**, 527–655 (2002).

[54] P. Piecuch and R. J. Bartlett, "Eomxcc: A new coupled-cluster method for electronic excited states," in *Advances in Quantum Chemistry*, Vol. 34 (Elsevier, 1999) pp. 295–380.

[55] J. F. Stanton and R. J. Bartlett, "The equation of motion coupled-cluster method. a systematic biorthogonal approach to molecular excitation energies, transition probabilities, and excited state properties," J. Chem. Phys. **98**, 7029–7039 (1993).

[56] D. C. Comeau and R. J. Bartlett, "The equation-of-motion coupled-cluster method. applications to open-and closed-shell reference states," Chem. Phys. Lett. **207**, 414–423 (1993).

[57] S. Kambalapalli and J. V. Ortiz, "Solvated Succinate Dianion: Structures, Electron Binding Energies, and Dyson Orbitals," J. Phys. Chem. A **107**, 10360–10369 (2003).

[58] A. Guevara-García, A. Martínez, and J. V. Ortiz, "Electron binding energies and Dyson orbitals of $Al_5O_m^-$ (m=3,4,5) and $Al_5O_5H_2^-$," J. Chem. Phys. **127**, 234302 (2007).

[59]V. V. Zakjevskii, S. J. King, O. Dolgounitcheva, V. G. Zakrzewski, and J. V. Ortiz, "Base and phosphate electron detachment energies of deoxyribonucleotide anions." J. Am. Chem. Soc. **128**, 13350–13351 (2006).

[60]O. Dolgounitcheva, V. G. Zakrzewski, and J. V. Ortiz, "Electron propagator calculations show that alkyl substituents alter porphyrin ionization energies." J. Am. Chem. Soc. **127**, 8240–8241 (2005).

[61]O. Dolgounitcheva, V. G. Zakrzewski, and J. V. Ortiz, "Ab initio electron propagator calculations on the ionization energies of free base porphine, magnesium porphyrin, and zinc porphyrin." J. Phys. Chem. A **109**, 11596–11601 (2005).

[62]S. Canuto, K. Coutinho, B. J. C. Cabral, V. G. Zakrzewski, and J. V. Ortiz, "Delocalized water and fluoride contributions to Dyson orbitals for electron detachment from the hydrated fluoride anion." J. Chem. Phys. **132**, 214507 (2010).

[63]O. Dolgounitcheva, V. G. Zakrzewski, and J. V. Ortiz, "Ionization Energies and Dyson Orbitals of Thymine and Other Methylated Uracils," J. Phys. Chem. A **106**, 8411–8416 (2002).

[64]J. V. Ortiz, "Dyson-orbital concepts for description of electrons in molecules," J. Chem. Phys. **153**, 070902 (2020), https://doi.org/10.1063/5.0016472.

[65]M. Díaz-Tinoco, H. H. Corzo, F. Pawłowski, and J. Ortiz, "Do dyson orbitals resemble canonical hartree–fock orbitals?" Mol. Phys. **117**, 2275–2283 (2019).

[66]M. Díaz-Tinoco, H. Corzo, and J. Ortiz, "Electron propagator methods for vertical electron detachment energies of anions: Benchmarks and case studies," J. Chem. Theory Comput. **14**, 5881–5895 (2018).

[67]H. H. Corzo and J. V. Ortiz, "Electron propagator theory: Foundations and predictions," in *Advances in Quantum Chemistry*, Vol. 74 (Elsevier, 2017) pp. 267–298.

[68]H. H. Corzo and J. Ortiz, "Electron propagators based on generalised density operators," Mol. Phys. **115**, 545–551 (2017).

[69]O. Goscinski and P. Lindner, "Natural spin-orbitals and generalized overlap amplitudes," J. Math. Phys. **11**, 1313–1317 (1970).

[70]J. Linderberg and Y. Öhrn, *Propagators in quantum chemistry* (John Wiley & Sons, 2004).

[71]R. L. Martin and E. R. Davidson, "Halogen atomic and diatomic 1s hole states," Phys. Rev. A **16**, 1341–1346 (1977).

[72] L. Cederbaum and W. Domcke, "Theoretical aspects of ionization potentials and photoelectron spectroscopy: A green's function approach," Adv. Chem. Phys. **36**, 205–344 (1977).

[73] J. Ortiz, "Toward an exact one-electron picture of chemical bonding," Adv. Quantum Chem. **35**, 33–52 (1999).

[74] A. I. Krylov, "From orbitals to observables and back," J. Chem. Phys. **153**, 080901 (2020).

[75] J. V. Ortiz, "Electron propagator theory: an approach to prediction and interpretation in quantum chemistry," Wiley Interdiscip. Rev.: Comput. Mol. Sci. **3**, 123–142 (2012).

[76] A. T. Amos and G. G. Hall, "Single determinant wave functions," Proc. R. Soc. London, Ser. A **263**, 483–493 (1961).

[77] H. F. King, R. E. Stanton, H. Kim, R. E. Wyatt, and R. G. Parr, "Corresponding orbitals and the nonorthogonality problem in molecular quantum mechanics," J. Chem. Phys. **47**, 1936–1941 (1967).

[78] T. Koopmans, "Über die Zuordnung von Wellenfunktionen und Eigenwerten zu den einzelnen Elektronen eines Atoms," Z. Phys. **1**, 104–113 (1934).

[79] A. Szabo and N. S. Ostlund, *Modern quantum chemistry: introduction to advanced electronic structure theory* (Courier Corporation, 2012).

[80] P. Politzer and F. Abu-Awwad, "A comparative analysis of hartree-fock and kohn-sham orbital energies," Theor. Chem. Acc. **99**, 83–87 (1998).

[81] S. Hamel, P. Duffy, M. E. Casida, and D. R. Salahub, "Kohn–sham orbitals and orbital energies: fictitious constructs but good approximations all the same," J. Electron. Spectrosc. Relat. Phenom. **123**, 345–363 (2002).

[82] L. M. Thompson, H. Harb, and H. P. Hratchian, "Natural ionization orbitals for interpreting electron detachment processes," J. Chem. Phys. **144**, 204117 (2016).

[83] J. L. Mason, H. Harb, A. Abou Taka, A. J. McMahon, C. D. Huizenga, H. H. Corzo, H. P. Hratchian, and C. C. Jarrold, "Photoelectron spectra of $Gd_2O_2^-$ and non-monotonic photon-energy dependent variations in populations of close-lying neutral states," ChemRxiv (2020).

[84] A. Abou Taka, M. C. Babin, X. Sheng, J. A. DeVine, D. M. Neumark, and H. P. Hratchian, "Unveiling the coexistence of structural isomers in the hydrolysis of $ZrO_2$: A combined computational and photoelectron spectroscopy study," ChemRxiv (2020).

[85] R. L. Martin, "Natural transition orbitals," J. Chem. Phys. **118**, 4775–4 (2003).

[86]Sylvester's determinant theorem shows that $\det(\mathbf{I}_m + \mathbf{AB}) = \det(\mathbf{I}_n + \mathbf{BA})$ where $\mathbf{A}$ is dimensioned $(m \times n)$ and $\mathbf{B}$ is dimensioned $(n \times m)$.

[87]J. J. Sylvester, "Xxxvii. on the relation between the minor determinants of linearly equivalent quadratic functions," The London, Edinburgh, and Dublin Philosophical Magazine and Journal of Science **1**, 295–305 (1851).

[88]T. Muir and W. H. Metzler, *A Treatise on the Theory of Determinants* (Courier Corporation, 2003).

[89]A. G. Akritas, E. K. Akritas, and G. I. Malaschonok, "Various proofs of sylvester's (determinant) identity," Mathematics and Computers in Simulation **42**, 585–593 (1996).

[90]M. J. Frisch, G. W. Trucks, H. B. Schlegel, G. E. Scuseria, M. A. Robb, J. R. Cheeseman, G. Scalmani, V. Barone, B. Mennucci, G. A. Petersson, H. Nakatsuji, M. Caricato, X. Li, H. P. Hratchian, A. F. Izmaylov, J. Bloino, B. Janesko, F. Lipparini, G. Zheng, J. L. Sonnenberg, W. Liang, M. Hada, M. Ehara, K. Toyota, R. Fukuda, J. Hasegawa, M. Ishida, T. Nakajima, Y. Honda, O. Kitao, H. Nakai, T. Vreven, J. A. Montgomery, Jr., J. E. Peralta, F. Ogliaro, M. Bearpark, J. J. Heyd, E. Brothers, K. N. Kudin, V. N. Staroverov, T. Keith, R. Kobayashi, J. Normand, K. Raghavachari, A. Rendell, J. C. Burant, S. S. Iyengar, J. Tomasi, M. Cossi, N. Rega, J. M. Millam, M. Klene, J. E. Knox, J. B. Cross, V. Bakken, C. Adamo, J. Jaramillo, R. Gomperts, R. E. Stratmann, O. Yazyev, A. J. Austin, R. Cammi, C. Pomelli, J. W. Ochterski, R. L. Martin, K. Morokuma, V. G. Zakrzewski, G. A. Voth, P. Salvador, J. J. Dannenberg, S. Dapprich, P. V. Parandekar, N. J. Mayhall, A. D. Daniels, O. Farkas, J. B. Foresman, J. V. Ortiz, J. Cioslowski, and D. J. Fox, Gaussian Development Version, Revision I.03+, Gaussian, Inc., Wallingford CT, 2014.

[91]R. Bauernschmitt and R. Ahlrichs, "Stability analysis for solutions of the closed shell kohn–sham equation," J. Chem. Phys. **104**, 9047–9052 (1996).

[92]R. Seeger and J. A. Pople, "Self-consistent molecular orbital methods. xviii. constraints and stability in hartree–fock theory," J. Chem. Phys. **66**, 3045–3050 (1977).

[93]H. P. Hratchian and H. B. Schlegel, "Finding minima, transition states, and following reaction pathways on ab initio potential energy surfaces," in *Theory and Applications of Computational Chemistry* (Elsevier, 2005) pp. 195–249.

[94]H. Harb and H. P. Hratchian, "Natural ionization orbitals v1.0," Code available at: https://github.com/HratchianGroup/niorep.

[95] J. M. Herbert and M. Head-Gordon, "Calculation of electron detachment energies for water cluster anions: an appraisal of electronic structure methods, with application to $(H_2O)_{20}^-$ AND $(H_2O)_{24}^-$." J. Phys. Chem. A **109**, 5217 – 5229 (2005).

[96] S. Li and D. A. Dixon, "Benchmark Calculations on the Electron Detachment Energies of $MO_3^-$ and $M_2O_6^-$ (M = Cr, Mo, W)," J. Phys. Chem. A **111**, 11908–11921 (2007).